Title

Quantifying water-use efficiency in plant canopies with varying leaf angle and density distribution.

Journal

Annals of Botany, 133(4)

Authors

Ponce de León, María
Bailey, Brian

Publication Date

2024-04-23

DOI

10.1093/aob/mcae018

Peer reviewed

Annals of Botany **133**: 605–620, 2024
https://doi.org/10.1093/aob/mcae018, available online at www.academic.oup.com/aob

ANNALS OF BOTANY
Nonprofit since 1887

Quantifying water-use efficiency in plant canopies with varying leaf angle and density distribution

María A. Ponce de León[1,*] and Brian N. Bailey[1]

[1]*Department of Plant Sciences, University of California, Davis, Davis, CA 95616, USA*
[*]*For correspondence. E-mail aponcedeleon@ucdavis.edu*

Received: 13 September 2023 Returned for revision: 10 January 2024 Editorial decision: 2 February 2024 Accepted: 7 February 2024

• **Background and Aims:** Variation in architectural traits related to the spatial and angular distribution of leaf area can have considerable impacts on canopy-scale fluxes contributing to water-use efficiency (WUE). These architectural traits are frequent targets for crop improvement and for improving the understanding and predictions of net ecosystem carbon and water fluxes.
• **Methods:** A three-dimensional, leaf-resolving model along with a range of virtually generated hypothetical canopies were used to quantify interactions between canopy structure and WUE by examining its response to variation of leaf inclination independent of leaf azimuth, canopy heterogeneity, vegetation density and physiological parameters.
• **Key Results:** Overall, increasing leaf area index (LAI), increasing the daily-averaged fraction of leaf area projected in the sun direction (G_{avg}) via the leaf inclination or azimuth distribution and increasing homogeneity had a similar effect on canopy-scale daily fluxes contributing to WUE. Increasing any of these parameters tended to increase daily light interception, increase daily net photosynthesis at low LAI and decrease it at high LAI, increase daily transpiration and decrease WUE. Isolated spherical crowns could decrease photosynthesis by ~60 % but increase daily WUE ≤130 % relative to a homogeneous canopy with equivalent leaf area density. There was no observed optimum in daily canopy WUE as LAI, leaf angle distribution or heterogeneity was varied. However, when the canopy was dense, a more vertical leaf angle distribution could increase both photosynthesis and WUE simultaneously.
• **Conclusions:** Variation in leaf angle and density distributions can have a substantial impact on canopy-level carbon and water fluxes, with potential trade-offs between the two. These traits might therefore be viable target traits for increasing or maintaining crop productivity while using less water, and for improvement of simplified models. Increasing canopy density or decreasing canopy heterogeneity increases the impact of leaf angle on WUE and its dependent processes.

Key words: Biophysical model, heterogeneous canopies, leaf angle distribution, three-dimensional model, water-use efficiency.

INTRODUCTION

The potential amount of sunlight that can be intercepted by plants is determined primarily by the angle of leaves relative to incoming beams of solar radiation and by the density and arrangement of neighbouring leaves in space, which is commonly termed canopy structure. The leaf angle can be characterized by the leaf inclination, defined as the angle between the leaf surface normal and the vertical direction, and the leaf azimuthal angle, defined as the polar angle of the projection of the leaf normal on a horizontal plane (Ross, 1981). For a single layer of leaves with no self-shading, the potential light flux that can be absorbed is determined by the fraction of the total leaf area projected in the direction of incoming beams of radiation (Ross, 1981). Neglecting diffuse radiation, a leaf layer with lamina biasing towards a horizontal orientation will intercept more radiation when the sun is near the zenith and less when it is near the horizon (Ehleringer and Werk, 1986; Ezcurra *et al.*, 1991). Adding multiple leaf layers can significantly affect the overall canopy-level behaviour in response to variation in leaf angle (Falster and Westoby, 2003). For example, a canopy with leaves biasing towards the vertical will decrease interception in the upper canopy layers, leading to more transmission of light into the lower canopy and potentially to the ground depending on the overall canopy density (de Wit, 1965).

Absorbed solar radiation drives a wide range of biophysical processes dependent on light or temperature, including photosynthesis, transpiration and metabolism. At the leaf level, the response of photosynthesis to light is highly non-linear. Rates of net photosynthesis tend to increase sharply with increasing light at low light and can be nearly constant or decrease with increasing light at high light (Ort, 2001). The transpiration flux for a leaf typically increases as light increases (Wise *et al.*, 1990), with the slope potentially decreasing because of stomatal closure as radiation-driven temperature increases at high light. The ratio of net photosynthesis to transpiration flux for a leaf, which we term here the water-use efficiency (WUE), tends to increase as light intensity increases and reach an optimum at the point where photosynthesis begins to saturate with light (Kao *et al.*, 1998).

At the canopy level, self-shading attributable to multiple leaf layers can be significant, which can change the emergent whole-canopy-level behaviour of processes related to WUE. Increasing leaf area or having a leaf angle distribution that biases towards the horizontal tends to intercept more light overall, but can potentially decrease total canopy photosynthetic capacity (Digrado *et al.*, 2020) and WUE owing to excessive shading in the lower canopy (Srinivasan *et al.*, 2017). Canopy architectures with more erect leaves, especially at the top of the canopy, can lead to increased light penetration and an overall increase in canopy photosynthesis and WUE in comparison to horizontally biased leaf angles (Forseth and Ehleringer, 1983; James and Bell, 2000; Long *et al.*, 2006). Although many canopy traits are capable of influencing photosynthesis and WUE, Digrado *et al.* (2020) found that for cowpea crops, leaf area index (LAI) and leaf area exposure had the largest influence on these processes compared with other traits, such as the number of nodes, stem length and shoot mass.

Understanding the crucial traits underpinning plant WUE is important for a wide range of applications spanning basic biology, agricultural production and plant systems modelling. A primary goal of modern agriculture is to increase or maintain productivity while reducing required inputs, such as water (i.e. higher WUE). This could be accomplished by breeding for cultivars with high photosynthetic capacity (Condon *et al.*, 2004) or by selecting lines with leaves that tend towards the vertical rather than towards the horizontal, which has been done in wheat to increase yields (Richards *et al.*, 2019). For existing cultivars, management practices such as pruning and thinning have been proposed as a means by which WUE can be increased (Forrester *et al.*, 2012; Jin *et al.*, 2018).

Despite the known potential for increasing WUE through variation in plant architectural traits, accurately quantifying or predicting WUE in the presence of many confounding variables has remained a challenge. Our understanding of and ability to measure plant biophysical processes at the leaf level has advanced rapidly owing to portable infrared gas analysers (Long *et al.*, 1996; Watanabe *et al.*, 2005; McPherson, 2007; Song *et al.*, 2013), yet these instruments are low throughput and produce instantaneous measurements for single leaves. Thus, it is difficult to determine how these measurements scale to the canopy level, especially in heterogeneous and anisotropic canopies. Tower-based flux measurements can quantify canopy-scale WUE (e.g. Knauer *et al.*, 2018; Nelson *et al.*, 2020), but generally do not allow for systematic variation in structural and physiological parameters because there are usually many confounding covariates when comparing across space and time. Models have been used as an alternative for scaling up leaf-level processes to the canopy level for many decades. However, in traditional land surface models, the canopy is usually represented in these models through simplified equations based on assumptions of horizontal homogeneity and often leaf isotropy (Jones *et al.*, 1991, 2003; Humphries and Long, 1995; Lloyd *et al.*, 1995; Foley *et al.*, 1996; Sellers *et al.*, 1996; De Pury and Farquhar, 1997; Wang and Leuning, 1998). Instead of resolving the fluxes at the leaf level, these simplified models calculate average fluxes for the whole canopy, for horizontal layers of the canopy or for leaf angle classes within layers of the canopy. Thus, there is limited knowledge of the net effect of canopy heterogeneity and anisotropy on these biophysical processes.

High-resolution, three-dimensional (3D) models of plant structure coupled with physically based models of plant function have the capability of realistically representing the 3D arrangement of leaves in space and associated biophysical processes across a wide range of plant canopies with varying levels of leaf anisotropy and heterogeneity. Potential applications are diverse and include energy transfer (e.g. Pearcy and Yang, 1996; Chelle and Andrieu, 1998; Henke and Buck-Sorlin, 2017; Bailey, 2018, 2019), turbulent transport processes (Mahaffee *et al.*, 2023) and photosynthesis (Song *et al.*, 2013; Wang *et al.*, 2017; Bailey and Kent, 2021). Previous work by Le Roux *et al.* (2001) used a 3D model to study the within-crown variability in WUE in a low-density orchard and found large short-term variation in horizontal WUE gradients within isolated crowns, suggesting potential importance of crown-level canopy structure. However, to our knowledge, 3D models have not been used to study the canopy-scale effect of heterogeneity and anisotropy on WUE.

In this work, we used a detailed 3D leaf-resolving canopy model, Helios (Bailey, 2019), to independently study the effects of interacting plant architectural traits on WUE and related processes. The spatially explicit nature of the 3D, leaf-resolving modelling approach allowed for the examination of WUE in response to variation of leaf inclination independent of leaf azimuth, canopy heterogeneity and canopy density (in m^2 leaf per m^3 canopy). We sought to determine cases in which the increase in canopy-absorbed radiation could significantly alter WUE through variation in the distribution of leaf area and angle. To understand the dependence between canopy structure and WUE, we varied parameters driving photosynthesis and transpiration. It was hypothesized that the degree to which leaf angle can affect spatial and temporal variations in WUE is strongly dependent on the spatial distribution and density of leaf area, such that a given leaf angle distribution could either increase or decrease WUE depending on the distribution of leaf area. It was additionally hypothesized that for cases with the same canopy density, the effect of leaf angle variation will increase in heterogeneous canopies.

MATERIALS AND METHODS

Model description

Leaf-absorbed radiation flux, leaf surface temperature (T_{leaf}), leaf transpiration flux (E_{leaf}) and leaf net photosynthetic flux (A_{leaf}) were simulated for a range of homogeneous and heterogeneous canopies using the Helios software (Bailey, 2019). Helios is a 3D plant modelling framework that simulates these biophysical processes at sub-leaf scales such that the entire plant/canopy geometry is fully resolved down to the scale of shadows. The geometry of leaves and the ground surface are represented by a mesh of rectangular patch elements. The model equations described below are applied for every patch element in the simulated domain, then aggregated to determine whole-canopy values (see 'Leaf angle distributions' section). The Helios sub-models used for this study were solar position and incident environmental flux models, radiation transport, surface energy balance, stomatal conductance and

photosynthesis. Each of these sub-models is described in detail in Bailey (2019), and only a brief overview is described below, with details given when specifically relevant to this study.

The solar position/flux sub-model calculates the incoming direct and diffuse solar radiation flux above the canopy using the REST-2 model of Gueymard (2008) and calculates the incoming diffuse longwave radiation flux from the sky using the model of Prata (1996). To calculate the position of the sun and radiative fluxes, this sub-model requires specification of the site longitude, latitude, offset from Universal Coordinated Time (UTC), atmospheric pressure, air temperature (T_{air}), atmospheric turbidity coefficient, relative humidity and Julian day of the year.

The radiation transport sub-model calculates the absorbed radiation for every geometric object in the simulated domain and terrestrial emission based on the above-specified ambient radiative fluxes using a reverse ray-tracing approach (Bailey, 2018). For this sub-model, information on surface reflectivity, transmissivity and emissivity of the geometric objects in the simulated domain needs to be specified.

The surface energy balance sub-model calculates the leaf temperature that balances the leaf energy budget equation, which is a balance between energy fluxes of radiation, sensible heat and latent heat (L) as described by Bailey (2019). The net radiative flux for each leaf element was calculated by the radiation transport model as introduced above. The leaf boundary-layer conductance to heat (g_H; in mol m^{-2} s^{-1}) was calculated using the Polhausen equation (Schuepp, 1993) as:

$$g_H = (2 \times 0.135)\sqrt{\frac{U}{d}}, \tag{1}$$

where U is the wind speed outside of the leaf boundary layer, d is the characteristic dimension of the leaf, and the factor of two accounts for (symmetric) convective heat transfer from both sides of the leaf. The ground boundary-layer conductance was calculated as in the paper by Kustas and Norman (1999):

$$g_H = 0.1662 + 0.4987\ U. \tag{2}$$

The latent heat flux (in W m^{-2}) was calculated for leaf surfaces as:

$$L = \lambda g_w \frac{e_s(T_{leaf}) - e_s(T_{air})\ RH}{P_{atm}}, \tag{3}$$

where λ = 44 000 J mol^{-1} is the latent heat of vaporization for water, g_w (in mol m^{-2} s^{-1}) is the conductance to water vapour from the sub-surface air spaces (i.e. stomatal cavity) to the air outside the surface boundary layer, $e_s(T_{leaf})$ (in kPa) is the saturated water vapour pressure evaluated at the leaf element surface temperature, and $e_s(T_{air})$ (in kPa) is the ambient air saturation vapour pressure.

The value of g_w was calculated, accounting for the serial pathway for water vapour diffusion through the stomata and boundary layer, as:

$$g_w = n_s \frac{(1.08\ g_H/2)\ g_S}{(1.08\ g_H/2) + g_S}, \tag{4}$$

where the factor 1.08 is based on the higher rate of diffusion of water vapour in the air compared with heat, g_S (in mol m^{-2} s^{-1}) is the stomatal conductance to water vapour, and n_s = 1 is the number of leaf sides with stomata (i.e. assumed hypostomatous). The stomatal conductance was modelled following Buckley *et al.* (2012) as:

$$g_S = \frac{E_m\,(Q_{leaf} + i_0)}{k + b\ Q_{leaf} + (Q_{leaf} + i_0)\ D}, \tag{5}$$

where Q_{leaf} (in µmol m^{-2} s^{-1}) is the absorbed leaf photosynthetically active radiation flux and D (in mmol mol^{-1}) is the vapour pressure deficit (VPD) between the intercellular leaf air spaces and leaf surface. The coefficients E_m, i_0, k, and b are semi-empirical.

The leaf transpiration flux (in mmol m^{-2} s^{-1}) was calculated from the latent heat term as:

$$E_{leaf} = 1000\left(\frac{L}{\lambda}\right). \tag{6}$$

The photosynthesis sub-model calculates the net leaf CO_2 flux, A_{leaf} (in µmol m^{-2} s^{-1}), as the minimum of two potential capacities to fix carbon, following the mechanistic biochemical model of Farquhar *et al.* (1980), expressed as:

$$A_{leaf} = \left(1 - \frac{\Gamma^*}{C_i}\right)\min\ \{W_c,\ W_j\} \quad - R_d, \tag{7}$$

where Γ^* (in µmol mol^{-1}) is the photosynthetic CO_2 compensation point in the absence of dark respiration, C_i (in µmol mol^{-1}) is the intercellular CO_2 concentration, W_c (in µmol m^{-2} s^{-1}) is the rate limited by Rubisco, W_j (in µmol m^{-2} s^{-1}) is the rate limited by RuBP regeneration, and R_d (in µmol m^{-2} s^{-1}) is the dark respiration rate.

The values of C_i and A_{leaf} were both calculated in Eqn (7) with the CO_2 diffusion equation, $A_{leaf} = 0.75 g_w (C_a - C_i)$, which is solved numerically for C_i using the secant method. The factor of 0.75 is based on the lower diffusion of CO_2 in the air in comparison to water vapour (Campbell and Norman, 1998), and C_a (in µmol mol^{-1}) is the CO_2 concentration of air outside of the leaf boundary layer.

The value of W_c was calculated as:

$$W_c = \frac{V_{cmax} C_i}{C_i + K_c\left(1 + \frac{O}{K_o}\right)}, \tag{8}$$

where V_{cmax} (in µmol m^{-2} s^{-1}) is the maximum carboxylation rate, O is oxygen concentration (in µmol mol^{-1}), K_o (in µmol mol^{-1}) is the Michaelis–Menten constant for O_2, and K_c (in µmol mol^{-1}) is the Michaelis–Menten constant for CO_2.

The value of W_j was calculated as:

$$W_j = \frac{J\,C_i}{4\,C_i + 8\ \Gamma^*}, \tag{9}$$

with the potential electron transport rate, J (in µmol m^{-2} s^{-1}), calculated as

$$J = \frac{\alpha\ J_{max}\ Q_{leaf}}{\alpha\ Q_{leaf} + J_{max}}, \tag{10}$$

where J_{max} (in µmol m^{-2} s^{-1}) is the maximum electron transport rate, and α is a unitless light response rate parameter.

The temperature dependence of Γ^*, K_c, K_o, R_d, V_{cmax} and J_{max} was included, following the description given by Bernacchi *et*

al. (2001) and Bernacchi *et al.* (2003) (see also Bailey, 2019, for details on the specific implementation). Helios v.1.2.65 was used to perform the simulations in this work, for which source code can be downloaded from https://www.github.com/PlantSimulationLab/Helios.

Integration of leaf fluxes

Instantaneous photosynthetically active radiation (PAR) interception for the whole canopy (Q) was calculated from the leaf PAR interception on a per unit ground area basis as:

$$Q = \frac{\sum_{i=1}^{N_l} a_{l,i}\, Q_{\text{leaf},i}}{a_g}, \tag{11}$$

where N_l is the number of leaf elements in the simulated canopy, $a_{l,i}$ is the one-sided surface area of the i^{th} leaf element, and a_g is the total ground surface area occupied by the canopy. The daily integrated Q_c was calculated based on instantaneous values at time step (Δt) up to time n as:

$$Q_c = \sum_{i=1}^{n} Q_i\ \Delta \text{t}, \tag{12}$$

where Q_i is the instantaneous whole-canopy flux at the i^{th} time step.

Instantaneous WUE for the whole canopy [in μmol CO_2 (mmol H_2O)$^{-1}$] was calculated as the ratio of instantaneous whole-canopy fluxes of photosynthesis (A) and instantaneous whole-canopy fluxes of transpiration (E) on a per unit ground area basis as:

$$\text{WUE} = \frac{A}{E}, \tag{13}$$

$$A = \sum_{i=1}^{N_l} \frac{a_{l,i}\, A_{\text{leaf},i}}{a_g}, \tag{14}$$

$$E = \sum_{i=1}^{N_l} \frac{a_{l,i}\, E_{\text{leaf},i}}{a_g}, \tag{15}$$

where $A_{\text{leaf},i}$ is the net CO_2 flux of the i^{th} leaf element and $E_{\text{leaf},i}$ is the transpiration flux of the i^{th} leaf element.

The daily integrated canopy water-use efficiency (WUE_c) was calculated as the ratio of daily integrated whole-canopy fluxes of A_c and E_c, as:

$$\text{WUE}_c = \frac{A_c}{E_c}, \tag{16}$$

$$A_c = \sum_{i=1}^{n} A_i\ \Delta t, \tag{17}$$

$$E_c = \sum_{i=1}^{n} E_i\ \Delta t, \tag{18}$$

where A_i and E_i are the instantaneous whole-canopy photosynthetic and transpiration fluxes at the i^{th} time step.

Instantaneous canopy temperature (T_s) was calculated from the patch temperature weighted by patch area for each leaf.

Weather data

The incoming radiation was calculated based on an assumed virtual site longitude (121.76°W), latitude (38.55°N), offset from UTC (7 h), atmospheric pressure (101 000 Pa), air temperature and humidity (variable), atmospheric turbidity coefficient (0.01) and Julian day of the year (153). The short-wave radiation was assumed to be partitioned between the PAR band (<700 nm) and the solar near-infrared band (>700 nm), 47 %, and 53 %, respectively. For this study, all solar energy was chosen to be collimated in the direction of the sun, and the sky was assumed to be cloudless. The number of direct rays used to sample each element was 500, and the number of diffuse rays per element was 1000. The radiation transport model recursive scattering depth was chosen to be two (Bailey, 2018).

The air temperature, relative humidity and wind speed were obtained as a 5-min average from the University of California Davis/National Oceanic and Atmospheric Administration (NOAA) local weather station at the Campbell Track in Davis, CA, USA (http://atm.ucdavis.edu/weather/uc-davis-weather-climate-station). During the study period (07:00–19:00 h), the average, maximum and minimum air temperature was 29.5, 35.4 and 18.8 °C, respectively. The average, maximum and minimum relative humidity was 0.35, 0.18 and 0.64, respectively, and the average wind speed was 3 m s^{-1}.

Test case set-up

To explore the effect of canopy structure on absorbed radiation, photosynthesis, transpiration and WUE, a range of hypothetical canopies were simulated with varying levels of leaf anisotropy, canopy heterogeneity and canopy density. Although Helios can represent arbitrarily complex canopy geometries (Bailey, 2019), simplified geometries were chosen for this study in order to isolate various contributors to WUE. Although the canopy cases do not correspond to any particular species, the chosen model input parameters (detailed below) could be thought of as most similar to hypostomatous broad-leafed C_3 species.

Leaf and ground parameters

The 3D geometry of the leaves was represented as a 10 × 10 uniform grid of planar squares, with the total surface area of each leaf being 0.0049 m^2. It was verified that the chosen leaf resolution was fine enough to resolve shadows (Supplementary Data Figs S1 and S2; Table S1), which is important for accurately determining canopy-scale fluxes (Bailey and Kent, 2021). The canopy height was set to 1 m. The reflectivity of leaves in the PAR band was set to 0.0855, the transmissivity in the PAR band to 0.0428, the reflectivity in the near-infrared band to 0.4455 and the transmissivity in the near-infrared band to 0.4041 (Ponce de León and Bailey, 2021). The leaf emissivity was assumed to be 0.96 (López *et al.*, 2012).

The baseline parameters at 25 °C set in the photosynthesis model were $V_{\text{cmax25}} = 78.5$ μmol m^{-2} s^{-1}, $\alpha = 0.45$, $R_{\text{d25}} = 2.12$

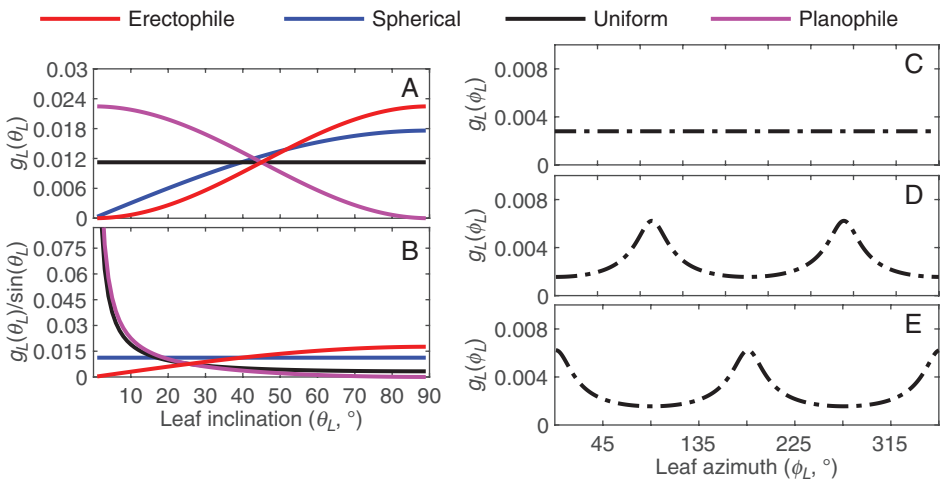

FIG. 1. Probability density function of sine-weighted (A) and actual (B) leaf inclination angle for canopy configuration cases with different distributions (spherical, uniform, planophile and erectophile) and of different leaf azimuth: isotropic (C), leaves biased towards E–W (D) and leaves oriented N–S (E). Each continuous line corresponds to a different leaf inclination angle distribution and each dashed line to a different leaf azimuth distribution. To depict differences among the leaf inclination angles more clearly, the *y*-axis was truncated in B.

μmol m^{-2} s^{-1} and J_{max25} = 133 μmol m^{-2} s^{-1}. The selected values of V_{cmax25} and J_{max25} are within the range of typical values for native plants (Walker *et al.*, 2014). These parameters were then varied to explore the dependence between canopy structure and WUE (see 'Analysis of physiological parameters' section). The value of V_{cmax25} was varied systematically between 20, 60 and 100 μmol m^{-2} s^{-1}. The corresponding value of J_{max25} for each V_{cmax25} value was calculated according to the empirical relationship:

$$\ln\left(J_{max25}\right) = a + c\,\ln\left(V_{cmax25}\right), \tag{19}$$

where a was set to 1.01 μmol m^{-2} s^{-1} and c to 0.89 (Walker *et al.*, 2014). The corresponding value of R_{d25} was calculated for each V_{cmax25} as:

$$R_{d25} = 0.027\ V_{cmax25}, \tag{20}$$

where 0.027 is the ratio of R_{d25} to V_{cmax25} for the chosen baseline parameter values.

The stomatal conductance model empirical coefficients i_0, k, and b were chosen to be equal to the values given by Bailey (2019), which were determined from measurements in *Prunus dulcis* at different combinations of light, temperature and ambient humidity, where i_0 = 38.48 μmol m^{-2} s^{-1}, k = 18 383 μmol m^{-2} s^{-1} mmol mol^{-1} and b = 49.68 mmol mol^{-1}. A value of E_m of 10 mmol m^{-2} s^{-1} was chosen as the baseline value, and a value of E_m of 20.4 mmol m^{-2} s^{-1}, which was measured by Bailey (2019), was also included in the study (see 'Analysis of physiological parameters' section).

The ground surface was represented as a 20 × 20 grid of rectangular patches. For all cases, periodic boundary conditions were applied in the horizontal directions to yield a horizontally infinite canopy. For the ground, the energy balance was applied by assuming no latent cooling attributable to water evaporation from the soil, and the heat storage term parameters were chosen as in the study by Ponce de León and Bailey (2021). For simplicity, the ground was considered to be black.

Leaf angle distributions

Hypothetical canopies were generated with varying leaf inclination and azimuth distributions. The leaf inclination distributions, $g_L(\theta_L)$, were generated by randomly sampling leaf angle inclinations from four different archetypal leaf angle distributions proposed by de Wit (1965) using the mathematical definitions of Goel and Strebel (1984) (Fig. 1A): spherical (isotropic); uniform (moderately biasing towards horizontal leaves); planophile (strongly biasing towards horizontal leaves); and erectophile (moderately biasing towards vertical leaves).

There is often confusion regarding these classical leaf angle distributions owing to the fact that their definitions usually include a pre-weighting of the leaf angle distribution by solid angle (i.e. multiplication by sin θ_L, where θ_L is the leaf inclination angle). This weighting by solid angle is necessary when integrating the probability distribution over θ_L in a spherical coordinate system. However, the unweighted probability density is given by $g_L(\theta_L)/\sin\theta_L$, which is plotted in Fig. 1B. Using this normalization, the expected isotropic distribution for 'spherical' leaves is achieved (i.e. constant probability with respect to θ_L). It can also be seen that the planophile distribution is much more strongly biased towards horizontal leaves than is the erectophile distribution towards vertical leaves. For reference, the fraction of leaf area projected in the vertical direction [$G(0)$; Ross, 1981] is $G(0) = 0.85$ for the planophile distribution and $G(0) = 0.42$ for the erectophile distribution, thus illustrating quantitatively that the planophile distribution is much further from the spherical distribution ($G = 0.5$) than the erectophile distribution. Fig. 1B also shows that the so-called uniform distribution is significantly biased towards horizontal leaves [$G(0) = 0.64$].

For each configuration, the leaf azimuth angles were sampled from a uniform distribution (azimuthally isotropic) independently of leaf inclination, and two contrasting anisotropic leaf azimuth distributions in which leaves were biased towards either the north–south (N–S) or east–west (E–W) directions. Note that in the spherical coordinate system, each azimuthal

angle has the same solid angle and thus there is no confusion with regard to solid angle weighting when integrating. Biasing leaves towards horizontal considerably increases the fraction of leaf area projected in the direction of the sun, G, relative to the spherical case ($G = 0.5$) throughout most of the day and might reduce it in the early and late daylight hours. The opposite is true for the vertically biased distribution (erectophile). Biasing leaf azimuth towards the E–W directions tends to increase G in the early and late hours of the day, whereas the N–S distribution has the opposite effect.

Case 1: homogeneous canopy

A set of homogeneous canopies were created with uniformly distributed leaves in space and varying leaf orientation distribution and LAI values. The number of leaves in the canopy was chosen to achieve four different LAI values: 0.5, 1, 3 and 5. The horizontal extent of the homogeneous canopy was 5 m × 5 m (but was extended infinitely through a periodic boundary condition). Homogeneous canopy geometries were generated for all combinations of the four LAI values and all leaf angle distribution cases described above (48 total cases). A sample visualization of the 3D distribution of modelled WUE for the homogeneous canopy case with spherical leaf inclination distribution and isotropic leaf azimuth is shown in Fig. 2A.

Case 2: heterogeneous canopy

Heterogeneous canopies were composed of spherical crowns filled with homogeneous vegetation arranged in a N–S row orientation and with three different row spacings: 1, 2 and 3 m. For all the cases, the spherical crowns had the same leaf area density of 5 $m^2\ m^{-3}$, but different canopy-level LAI attributable to the varying row spacing; 2.6 $m^2\ m^{-2}$ for 1 m row spacing, 1.3 $m^2\ m^{-2}$ for 2 m row spacing and 0.9 $m^2\ m^{-2}$ for 3 m row spacing. The radius of the spherical crowns was 0.5 m, the crown spacing within each row was 1 m, and there were 12 spherical crowns explicitly represented in total (but with periodic boundary conditions). The set-up of leaf inclination angle distribution was the same as case 1 (Fig. 1). The horizontal extent of the heterogeneous canopy varied based on the row spacing: for 1 m row spacing, 4 m × 3 m; for 2 m row spacing, 8 m × 3 m; and for 3 m row spacing, 12 m × 3 m. A sample visualization of the 3D distribution of WUE for the heterogeneous canopy case with 2 m row spacing and spherical leaf inclination distribution is shown in Fig. 2B.

Analysis of physiological parameters

To determine whether the effect of leaf angle varies owing to changes in leaf physiological parameters and to explore further the dependence between canopy density and WUE, parameters driving photosynthesis and transpiration were varied. For the analysis, V_{cmax25} was varied from 78.5 (reference) to 20, 60 and 100 μmol $m^{-2}\ s^{-1}$, R_{d25} was varied as a function of V_{cmax25} according to Eqn (20) from 2.1 (reference) to 0.5, 1.6 and 2.7 μmol $m^{-2}\ s^{-1}$, and J_{max25} was varied as a function of V_{cmax} according to Eqn (19) from 133 (reference) to 39.5, 105 and 165 μmol $m^{-2}\ s^{-1}$. Furthermore, parameter values of α were varied from 0.45 (reference) to 0.27 and 0.135, and values of E_m were varied from 10 (reference) to 6.2, 12.3 and 20.4 mmol $m^{-2}\ s^{-1}$. This analysis considered a subset of the homogeneous canopy cases that included different LAI values (0.5, 1, 3 and 5), with four different leaf angle distributions (spherical, uniform, planophile and erectophile, each with isotropic leaf azimuth).

RESULTS

Case 1: homogeneous canopy

Effect of leaf inclination distribution and LAI in a homogeneous canopy. As expected, daily PAR interception increased

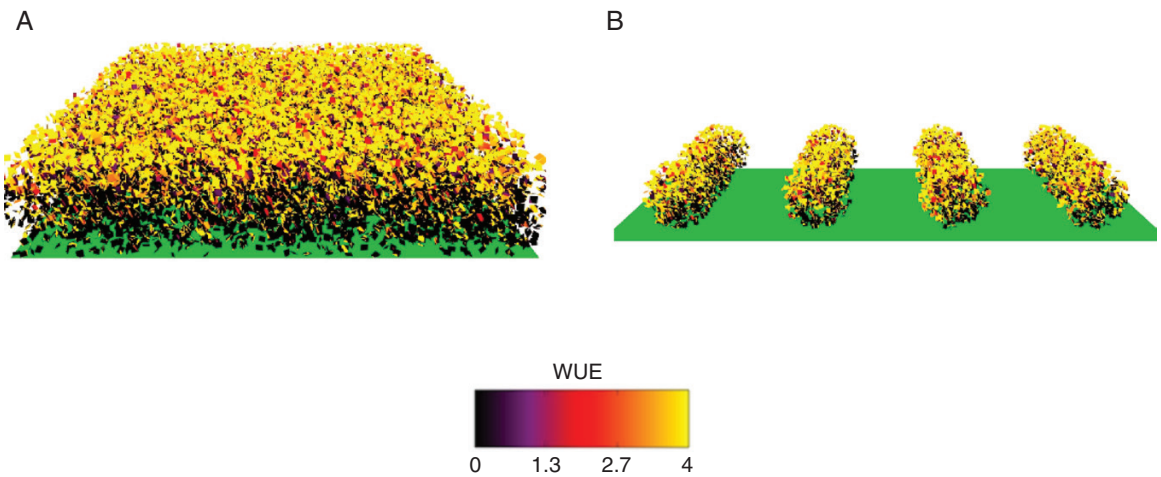

FIG. 2. Three-dimensional visualization of the canopy water-use efficiency [WUE; in μmol CO_2 (mmol H_2O)$^{-1}$] at 10:00 h for: (A) homogeneous canopy case (LAI of 5) and (B) heterogeneous canopy with 2 m row spacing, each with isotropic leaf inclination and azimuth distribution. Each leaf element is coloured based on a pseudocolour mapping between its calculated WUE and the colour scale shown in the figure. The ground was coloured green for contrast, because its WUE was undefined ($A = E = 0$). The canopies shown all had a leaf area density of 5 $m^2\ m^{-3}$.

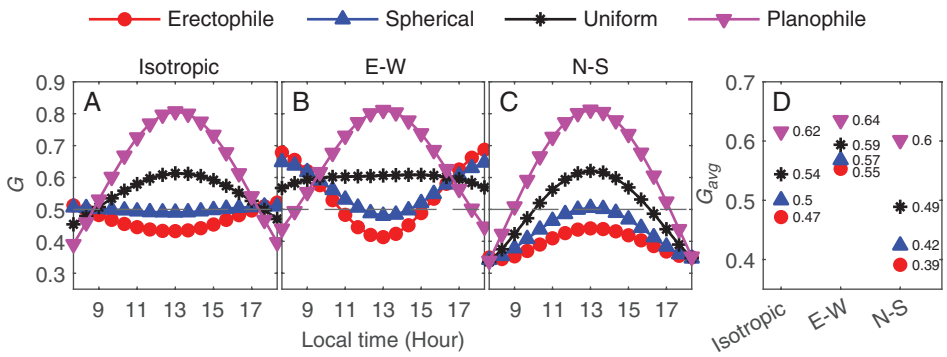

FIG. 3. Fraction of leaf area projected in the direction of the sun, G, for the virtual canopies with four different leaf inclination distributions (erectophile, spherical, uniform and planophile) and three different leaf azimuth distributions (isotropic, leaves biased towards E–W and leaves biased towards N–S). (A–C) Instantaneous G and (D) daily-averaged G (denoted as G_{avg}). The different line symbols correspond to leaf inclination distributions; sub-plots (in A–C) correspond to leaf azimuth distributions.

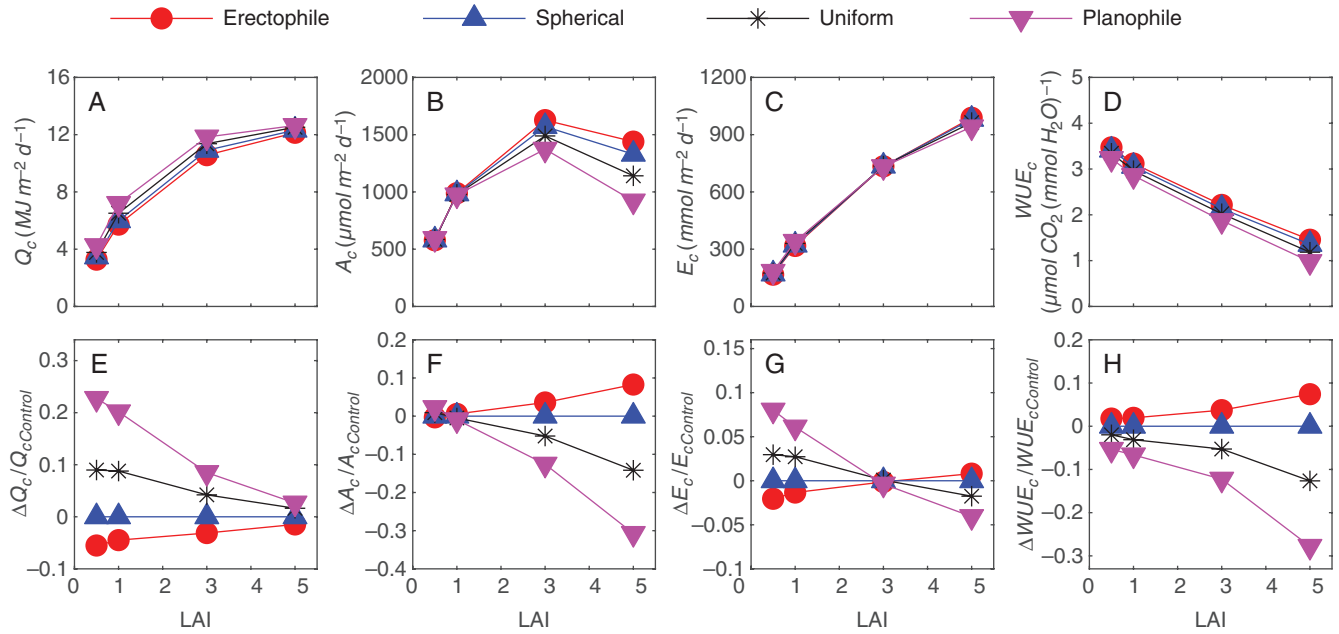

FIG. 4. Daily absorbed radiation (Q_c), photosynthesis (A_c), transpiration (E_c) and canopy water-use efficiency (WUE_c) for the homogeneous canopy cases with four different leaf inclination distributions (isotropic azimuth distribution: erectophile, spherical, uniform and planophile) and with four different leaf area index (LAI) values (0.5, 1, 3 and 5). (A–D) Daily integrated fluxes and (E–H) normalized difference (Δ) relative to the spherical leaf angle distribution (control case).

logarithmically as LAI was increased, with a diminishing rate of increase in Q_c as LAI increased. As the leaf angle distribution was increasingly biased towards horizontal leaves, the daily-averaged value of G_{avg} increased (Fig. 3A, D), which increased daily PAR interception (Fig. 4A). The effect of G on PAR interception at any instant during the day was relatively large, whereas the effect of G_{avg} on daily integrated PAR interception was comparatively small. The impact of leaf angle on Q_c diminished as LAI increased. There was a 28 % difference in Q_c between the erectophile and planophile leaf angle distributions when LAI = 0.5, which decreased to ~4 % when LAI = 5 (Fig. 4E). This is attributable to the fact that at high LAI, PAR absorption by the canopy approaches 100 % regardless of the value of G.

Although Q_c increased monotonically with LAI and G_{avg}, the trend in daily canopy photosynthesis, A_c, reversed as the canopy transitioned from low to high LAI (Fig. 4B). Below an LAI of approximately three, A_c increased as LAI increased and increased as G_{avg} increased (increasing bias towards horizontal leaves). Above an LAI of around three, A_c decreased as LAI or G_{avg} was increased, with the sensitivity of A_c to G_{avg} increasing as LAI increased (Fig. 4F). At low LAI, A_c is limited by the ability to capture light that would otherwise be lost to the ground, and thus higher LAI and Q_c increases daily photosynthesis in this regime. When the canopy is nearly optically thick at high LAI and little light is lost to the ground, A_c is limited by the shaded leaf area. As LAI becomes large, shaded leaf area becomes the majority fraction, which has

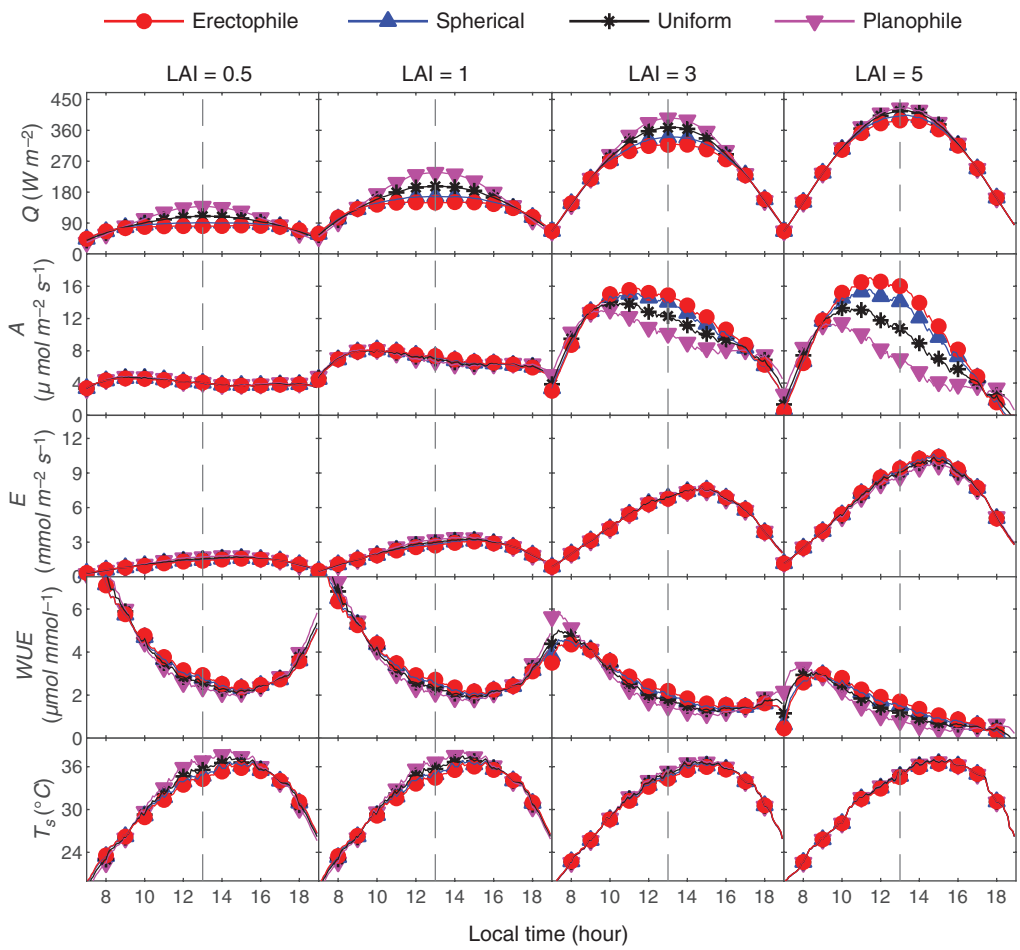

FIG. 5. Instantaneous whole-canopy fluxes of absorbed radiation (Q), photosynthesis (A), transpiration (E), water-use efficiency (WUE) and canopy temperature (T_s) for the homogeneous canopy cases with four different leaf angle distributions (isotropic azimuth distribution: erectophile, spherical, uniform and planophile) and with four different leaf area index (LAI) values (0.5, 1, 3 and 5). The dashed vertical line indicates the time at solar noon.

small or negative net photosynthetic fluxes owing to respiration. If the additional photosynthetic productivity of sunlit leaf area attributable to a marginal increase in LAI is less than the respiratory costs associated with shaded leaf area owing to the same increase in LAI, overall canopy photosynthesis will decrease. For the simulation parameters chosen here, this appears to occur for LAI ≥ 3.

Although LAI has a minimal impact on the photosynthetic flux of sunlit leaf area, G determines the average direct PAR flux on sunlit leaf area and thus determines the photosynthetic flux on sunlit leaf area. The response of leaf photosynthesis to light is logarithmic, meaning that the largest gains in photosynthesis from an increase in light are at lower light. When LAI is small, increasing G increases PAR intercepted by the canopy, which increases A_c. However, when LAI is large, increasing G increases the average PAR flux on sunlit leaves, which will increase leaf photosynthesis (assuming that the increase in PAR does not cause an excessive temperature increase that decreases photosynthesis) and also increases the fraction of shaded leaf area. If the respiratory costs associated with increased shaded leaf area outweigh the increases in photosynthesis owing to increased sunlit PAR flux, photosynthesis can decrease as G is increased.

The increase in daily canopy transpiration, E_c, with increasing LAI was nearly linear as the LAI increased from 0.5 to 5, with relatively close correspondence between E_c and Q_c (Fig. 4A, C). The effect of the leaf angle distribution via G_{avg} was relatively minimal ($\lesssim$10 % between erectophile and planophile distributions), and its effect was non-monotonic as LAI was varied (Fig. 4G). At low LAI, increasing G_{avg} increased E_c, whereas the opposite was true at the highest LAI of five. This appears to be attributable to the fact that the leaf angle distribution has an opposite effect on sunlit vs. shaded leaf area. At low LAI, increasing G_{avg} increases light capture by the canopy, which increases transpiration. At high LAI, there is a marginal increase in additional light capture when LAI is increased, and most additional leaf area added is shaded. Once the canopy is nearly optically thick, varying G_{avg} primarily affects the vertical distribution of energy rather than whole-canopy energy capture. Thus, increasing G_{avg} at high LAI tends to decrease E_c by concentrating energy in the upper canopy. However, sunlit and shaded leaf area both contribute positively to E_c. Thus, an optimum in E_c with respect to LAI does not occur.

Although the effect of LAI on A_c and G_{avg} on A_c and E_c was non-monotonic, the effect of both LAI and G_{avg} on daily canopy WUE was monotonic. The decrease in WUE_c with increasing

LAI was nearly linear (Fig. 4D). Increasing G_{avg} tended to decrease WUE_c, with this effect being negligible at an LAI of 0.5, and causing a ~35 % change in WUE_c between the erectophile and planophile canopies at LAI = 5 (Fig. 4H).

The instantaneous whole-canopy fluxes of Q tended to follow the magnitude of the incoming radiation flux, and the effect of the leaf angle distribution closely followed the diurnal trend in G (Figs 3A and 5). Similar to the increase in Q, A increased initially, but reached an optimum that occurred before solar noon owing to the flattening of the photosynthetic light response curve and stomatal closure with increasing VPD. The time of maximum absorbed radiation values happened around the same time (solar noon) for all canopies, but the time of maximal A varied among the different leaf angle cases. For instance, at high LAI, erectophile and spherical canopies had maximum A values between 10:00 and 11:00 h and uniform and planophile between 9:00 and 10:00 h. This is likely to be because, at high LAI, canopies with leaves tending towards horizontal become saturated with light earlier in comparison to canopies with leaves tending towards vertical.

The instantaneous whole-canopy fluxes of E increased as LAI increased and reached maximum values in the afternoon owing to the increase in VPD driven by ambient weather conditions. This corresponded to a similar diurnal peak in leaf temperature, T_s. These patterns suggest that E_c was more closely coupled with the ambient air than incident radiation for the chosen weather conditions. Overall, the effect of the leaf angle on E was small throughout the day, which is consistent with weak radiative coupling. In contrast, the effect of leaf angle on instantaneous whole-canopy fluxes of WUE varied slightly during the day and increased between 8:00 and 11:00 h at high LAI. The WUE values tended to be largest in the morning for all cases and were greater at low LAI. The lower WUE in the afternoon could be explained by the fact that E can increase continually for much of the day owing to a more linear response to light and increasing ambient VPD, whereas A begins to decline earlier in the day.

When LAI is low (Fig. 6A–E), variation in the leaf angle distribution causes a shift in the vertical profile relative to the spherical distribution that is fairly uniform with height and varies roughly according to the respective value of G (see Fig. 3A at 12:00 h). Absorbed radiation, net photosynthesis, transpiration, WUE and leaf temperature at a given height all tend to increase with respect to the spherical case according to G at low LAI.

When LAI < 1, there is minimal overlap between leaves, and thus the average absorbed radiation flux is nearly proportional to G. When LAI is much greater than one (Fig. 6F–J), similar behaviour is observed at 12:00 h in the upper canopy as for low LAI, but absorbed radiation tends to decrease relative to the spherical case with depth into the canopy when $G > 0.5$ and increase with depth when $G < 0.5$. There is some critical depth within the canopy at which the trend in absorbed radiation with G reverses. This crossover height is different for each of the variables considered in Fig. 6. It occurs at ~40 % of the canopy height for Q, 90 % of the canopy height for A, 60 % of the canopy height for E and 40 % of the canopy height for T_s. There was no crossover point for WUE, whereby WUE was always less than that of the spherical case when $G > 0.5$ and greater than the spherical case when $G < 0.5$. Variation in the crossover height relative to that of Q appears to be driven by the non-linearity of the response of the variables to light.

Effect of azimuthal anisotropy in a homogeneous canopy. Adding azimuthal anisotropy to the leaf angle distribution increased daily absorbed radiation by ≤11 % when leaf azimuths were biased towards E–W and reduced daily absorbed radiation by ≤13 % when biased towards N–S (Fig. 7). These differences agreed roughly with corresponding differences in G_{avg} (Fig. 3D). This suggested that more light could be captured

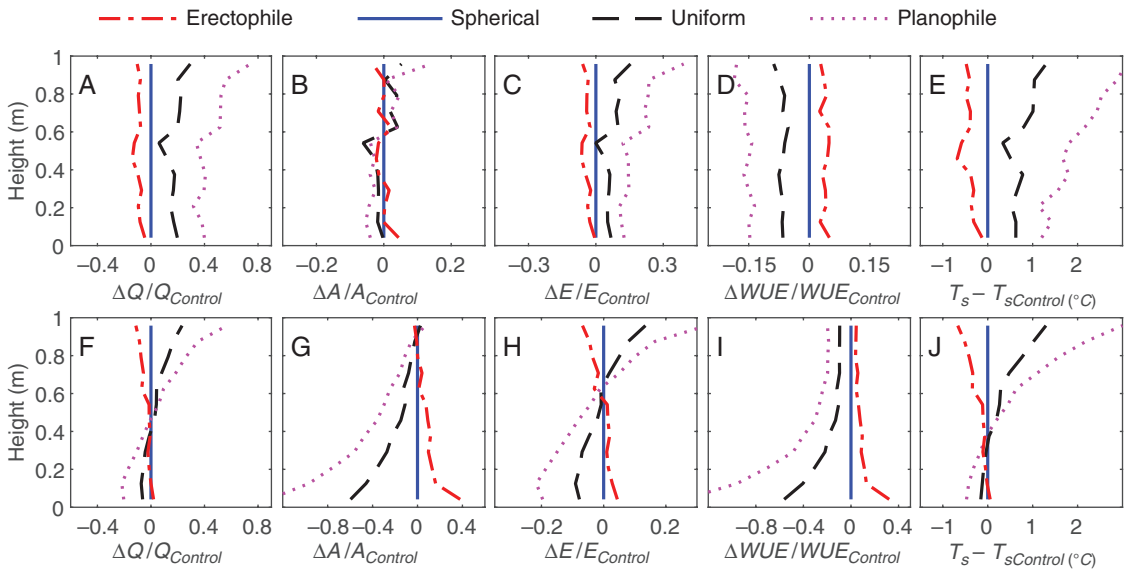

FIG. 6. Vertical profiles of normalized difference (Δ) relative to the control (spherical leaf angle distribution) of absorbed radiation (Q), photosynthesis (A), transpiration (E), water-use efficiency (WUE) and canopy temperature (T_s) for the homogeneous canopy cases with four different leaf angle distributions (erectophile, spherical, uniform and planophile) and two different leaf area index (LAI) values: 0.5 (A–E) and 3 (F–J) at 12:00 h. The canopy height is 1 m.

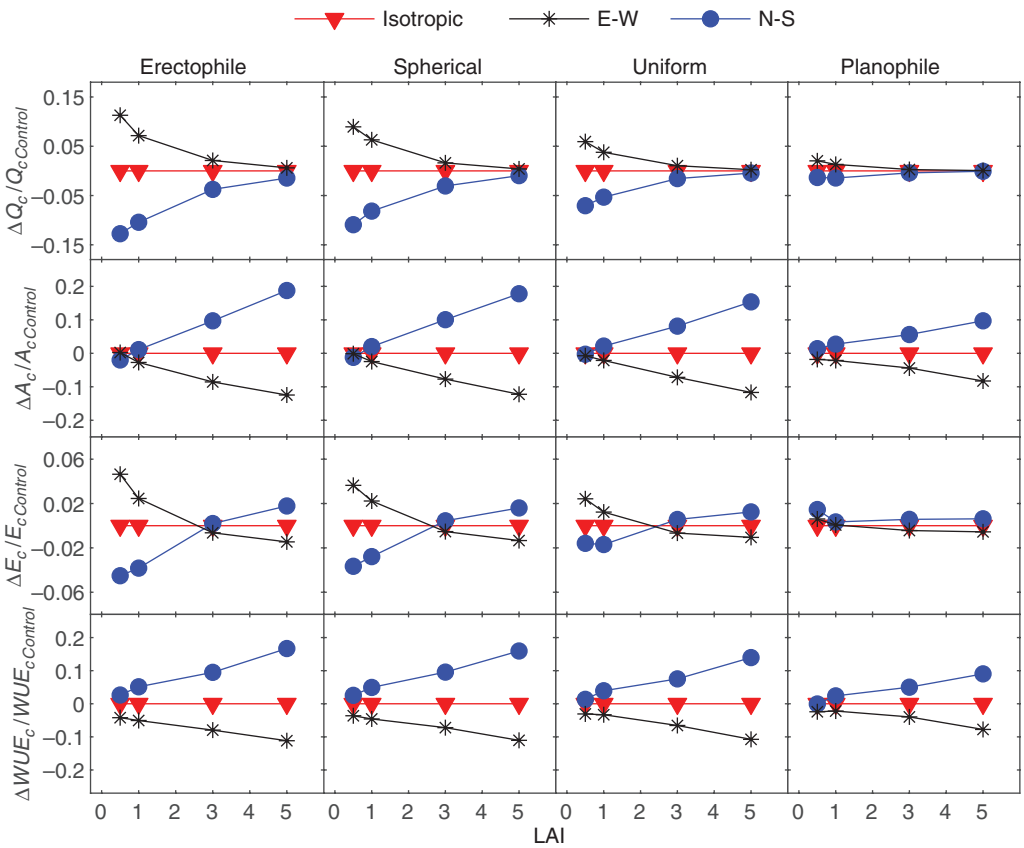

FIG. 7. Normalized difference (Δ) relative to the control (isotropic leaf azimuth) in daily integrated absorbed radiation (Q_c), photosynthesis (A_c), transpiration (E_c) and canopy water-use efficiency (WUE_c) owing to anisotropic leaf azimuth for the homogeneous canopy cases with four different leaf inclination distributions (erectophile, spherical, uniform and planophile) and with four different leaf area index (LAI) values (0.5, 1, 3 and 5).

over a day by E–W leaves than by N–S leaves by maximizing light interception in the early and late day, rather than only midday. The effect of azimuthal anisotropy on absorbed radiation diminished as LAI increased, as was also observed for leaf inclination anisotropy (Fig. 4), which is because denser canopies are able to absorb nearly all incoming light regardless of the value of G. Light interception also became less sensitive to azimuthal anisotropy as G_{avg} increased. This is because for a vertical leaf, changing azimuth has the possibility to move the leaf between full sun and full shade, whereas light interception of a horizontal leaf does not change with azimuth.

At high LAI, net photosynthesis was reduced relative to the azimuthally isotropic canopy when leaf azimuths were biased towards E–W and increased when azimuths were biased towards N–S. For the erectophile, spherical and uniform canopies, this trend reversed below an LAI of one or two. Daily-averaged G increased for leaf azimuths biased towards E–W and decreased for leaf azimuths biased towards N–S, with planophile G_{avg} being least affected by azimuthal anisotropy (Fig. 3D). It is expected that N–S-biased azimuths, for example, should have a similar effect as increasing LAI or G in the azimuthally isotropic cases (Fig. 4). This is in fact the trend that was observed: N–S-biased leaf azimuths increased photosynthesis at high LAI by allowing additional penetration of light into the canopy, whereas it decreased photosynthesis at low LAI owing to light lost to the ground. The effect was similar for transpiration and WUE. N–S-biased azimuths increased transpiration at high LAI and decreased transpiration at low LAI, with the planophile canopies having the least sensitivity to leaf azimuthal anisotropy. The WUE was increased with N–S-biased leaf azimuths, which was amplified with increasing LAI.

Case 2: effect of heterogeneity

The addition of canopy heterogeneity at constant leaf area density generally tended to decrease daily absorbed radiation, net photosynthesis and transpiration (Fig. 8). This is expected because there is less leaf area overall when leaf area per ground area is removed to increase heterogeneity. Increasing heterogeneity also increased WUE_c by ≤130 % relative to the homogeneous canopy, while decreasing daily net photosynthesis by ~60 % for the same case (Fig. 9). Although increasing plant spacing reduced both photosynthesis and transpiration owing to the associated reduction in overall leaf area per ground area, it tended to reduce transpiration more than photosynthesis. Most of the WUE gains occurred up to a plant spacing of ~2 m, beyond which there was little change in WUE.

Interestingly, there were cases in which removing canopy leaf area could increase net photosynthesis, A_c. This occurred for cases with leaves biased towards horizontal (uniform and planophile) when the canopy was transitioned from

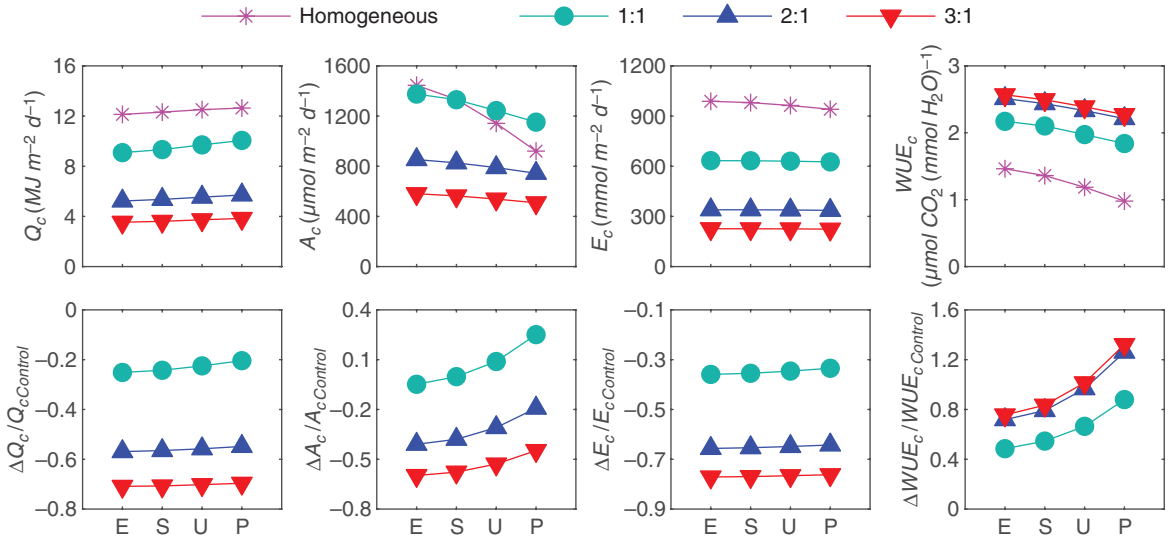

FIG. 8. Cumulative and normalized difference (Δ) relative to the control (homogeneous canopy case) of daily integrated absorbed radiation (Q_c), photosynthesis (A_c), transpiration (E_c) and canopy water-use efficiency (WUE_c) between a range of hypothetical heterogeneous canopies and their corresponding homogeneous canopy case. For the heterogeneous canopy cases, each line corresponds to cases with a different ratio between row spacing and canopy height (1 m). All canopies had the same leaf area density (5 m^2 m^{-3}) and included homogeneous and heterogeneous canopies with isotropic leaf inclination angle (S = spherical), and anisotropic leaf inclination (E = erectophile, U = uniform, P = planophile). The heterogeneous canopy was oriented in N–S rows and with three different row spacings: 1 m (canopy-level LAI = 2.6), 2 m (canopy-level LAI = 1.3) and 3 m (canopy-level LAI = 0.9).

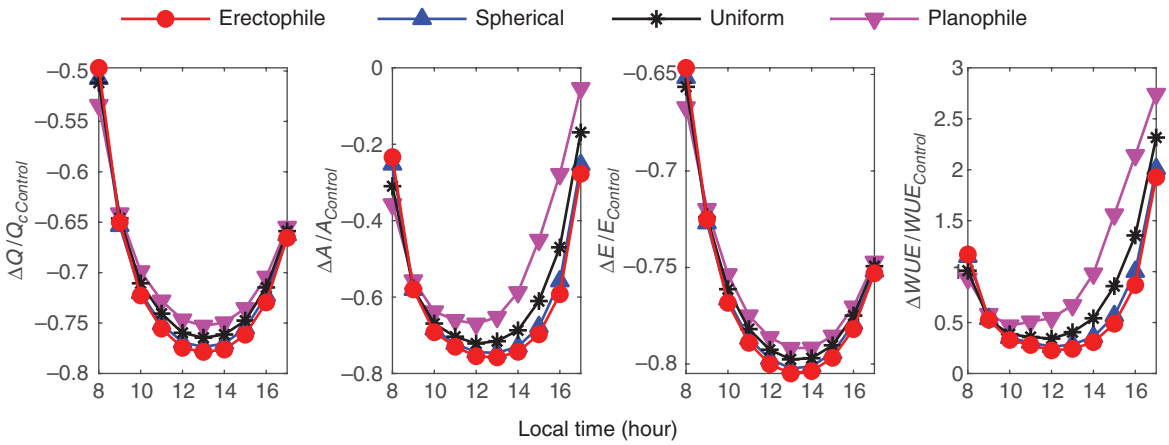

FIG. 9. Difference in instantaneous whole-canopy fluxes of absorbed radiation (Q), photosynthesis (A), transpiration (E) and water-use efficiency (WUE) between canopies with 3 m row spacing (canopy-level LAI = 0.9) and their corresponding homogeneous canopy (control) with the same leaf area density (5 m^2 m^{-3}). The canopies were oriented in N–S rows and included heterogeneous canopies with isotropic (spherical) and anisotropic leaf inclination angles (erectophile, uniform and planophile).

homogeneous to spherical crowns with the smallest row spacing. It is expected that this is attributable to a similar mechanism that created a decline in A_c in the homogeneous canopies when LAI was increased above three. Decreasing leaf area can result in a more efficient vertical light distribution when overall light absorption is high.

As heterogeneity increased, hourly whole-canopy fluxes of Q reduced per ground area, hence A and E decreased. However, WUE increased in the heterogeneous canopy compared with the homogeneous canopy by ≤270 % in the afternoon (Fig. 9). The largest increases in WUE as G was varied occurred in the horizontally biased leaf angle cases during the afternoon, when VPD was high. The effect of leaf inclination distribution on WUE was greater in the planophile leaf angle distribution case compared with the erectophile case because leaves in the planophile distribution are much more biased towards horizontal leaves than the erectophile distribution is biased towards vertical leaves (Fig. 1B).

Effect of physiological parameter variation

Variation in V_{cmax25} (and by extension, J_{max25} and R_{d25}) over nearly an order of magnitude had a significant effect on the impact of leaf angle on WUE_c (Fig. 10A–C). Increasing photosynthetic capacity via V_{cmax25} increases the magnitude of WUE_c, and the normalized values of WUE_c shown in Fig. 10A–C

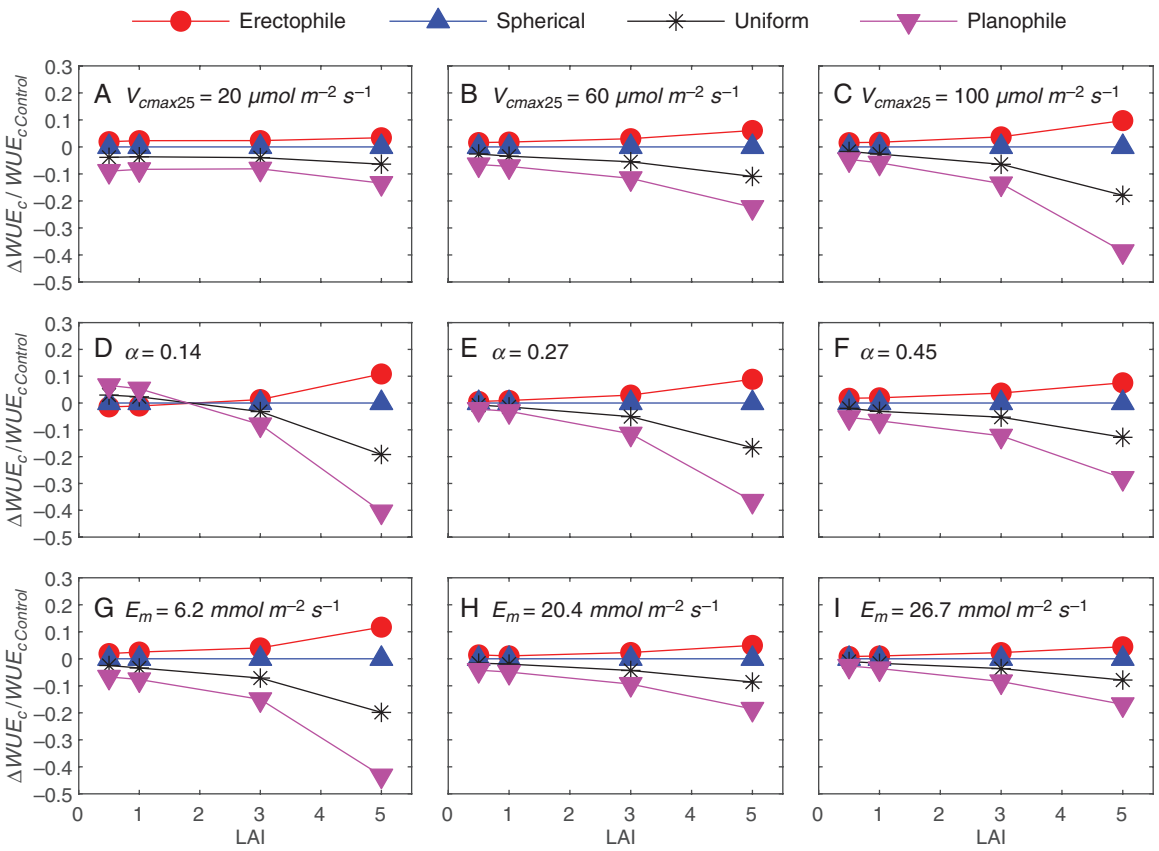

FIG. 10. Analyses of physiological parameters on water-use efficiency (WUE) when V_{cmax25} was varied from 78.5 (reference) to 20, 60 and 100 μmol m^{-2} s^{-1}, R_{d25} was varied according to Eqn (20) from 2.1 (reference) to 0.5, 1.6 and 2.7 μmol m^{-2} s^{-1}, and J_{max25} was varied according to Eqn (19) from 133 (reference) to 39.5, 105 and 165 μmol m^{-2} s^{-1}, respectively (A–C). The parameter value of α was reduced from 0.45 (reference) to 0.27 and 0.14 (D–F), and E_m was varied from 20.5 (reference) to 6.2, 12.3 and 26.7 mmol m^{-2} s^{-1} (G–I), respectively. The data plotted are for homogeneous canopies with leaf area index (LAI) of 0.5, 1, 3 and 5.

suggest that this increase has a relatively small impact on WUE at low V_{cmax25} across canopy cases and becomes increasingly significant at high V_{cmax25}.

Variation in the initial slope of the photosynthetic light response curve by changing the value of α did have a notable impact on the relationship between leaf angle and WUE_c (Fig. 10D–F). Varying α shifted the LAI value at which WUE_c increased or decreased relative to the spherical canopy when G_{avg} was varied. At low LAI, WUE_c increased with respect to the spherical canopy as G_{avg} increased. At some critical LAI value that decreased as α increased, this trend reversed. Increasing α causes photosynthesis to saturate at lower light levels. Thus, it is expected that decreasing α should cause an increase in WUE_c relative to the spherical canopy for leaf angle distributions biasing towards horizontal because it increases photosynthesis for the relatively large amount of low-light leaves in the lower canopy shaded by overlying leaf layers.

Increasing the maximum transpiration rate, E_m, decreased the sensitivity of WUE_c to leaf angle. Increasing E_m tends to increase the contribution of E_c to WUE_c. As was shown above, E_c is much less sensitive to the leaf angle distribution than A_c. Thus, it follows that increasing the contribution of E_c to WUE_c should decrease sensitivity of WUE_c to the leaf angle distribution.

DISCUSSION

Optima in WUE and photosynthesis with varying canopy architecture

Optimizing canopy structure to improve WUE has been proposed as an approach for producing more efficient crops under the changing climate (Drewry *et al.*, 2014; Srinivasan *et al.*, 2017; Hatfield and Dold, 2019). The results suggested that canopy structure could have a significant influence on both instantaneous and daily-integrated WUE. Within the range of homogeneous canopy cases considered, WUE varied among the cases by >100 % at a given hour and by nearly 35 % on a daily basis (mainly owing to LAI). High LAI tended to amplify the effect of leaf angle on WUE. Introducing canopy heterogeneity could create further increases in WUE.

Despite the pronounced effect of canopy structure on WUE, there did not appear to be a distinct optimum in WUE as LAI, leaf angle distribution or heterogeneity was varied. WUE decreased monotonically as LAI, G_{avg} or homogeneity was increased. Intuitively, it seems as though an instantaneous optimum in WUE_c could exist. At the leaf level, there is an optimum in WUE with respect to light at the so-called 'breakpoint' of the photosynthetic light response curve (Kao and Forseth, 1992). Thus, a leaf angle distribution that minimizes self-shading and

orients leaves such that radiative fluxes are near the breakpoint should be optimal. However, it might be that the limited flexibility of the four leaf angle distributions with isotropic azimuths did not find the optimum. It is also possible that an instantaneous optimum might exist, but that it cannot be maintained over an entire day without leaf solar tracking. This was estimated in slash pine and *Schima superba*, in which WUE_c was positively correlated with light, leaf temperature and VPD; however, after the breakpoint, WUE_c decreased with light, leaf temperature and VPD (Zhuang *et al.*, 2023).

Despite the lack of an observed WUE optimum, there was a distinct optimum in daily net photosynthesis, A_c, with varying LAI, as has been reported in previous experimental studies (Digrado *et al.*, 2020), which was attributable to the trade-off between productivity and respiratory costs via increasing leaf area. This optimum in A_c did not translate into an optimum in WUE because the denominator of WUE, E_c, continues to increase as LAI increases owing to the fact that sunlit and shaded leaf area contribute positively to E_c, whereas shaded leaf area tends to contribute negatively to A_c.

In our study, it was assumed that photosynthetic properties were uniform throughout the canopy. However, in real canopies, V_{cmax} would be smaller where light is lower, and respiration would tend to decline proportionately (Buckley *et al.*, 2013). This could potentially result in less of a carbon 'cost' owing to shaded leaves and could affect the optimum in A_c observed at moderate LAI (see Fig. 4). For instance, in corn at high density, removal of two leaves above the ear resulted in a 14 % increase in photosynthesis (Liu *et al.*, 2015). Despite this oversimplification based on uniform photosynthetic properties, our results for all the different leaf orientation cases agree with field observations in cowpea (Digrado *et al.*, 2020) and soybean (Srinivasan *et al.*, 2017), with an optimum in A_c at a similar LAI of around three.

Introducing canopy-scale heterogeneity monotonically increased WUE for an individual plant at the expense of whole-canopy productivity, and thus there was no clear optimum in WUE with varying plant density. However, in some cases there was an optimum in A_c. For the uniform and planophile leaf angle distributions, the smallest plant spacing (1:1) increased A_c relative to the homogeneous canopy, but then A_c declined for a 2:1 plant spacing (Fig. 8). This optimum is probably attributable to the same mechanism causing the optimum in A_c when LAI is varied in the homogeneous canopies. A small amount of heterogeneity allows for increased light penetration and increases the fraction of sunlit leaf area, and thus increases net photosynthesis. If this increase in net photosynthesis is larger than the overall reduction in total leaf area resulting from the heterogeneity, net photosynthesis can increase.

Leaf inclination angle anisotropy

Anisotropy in the leaf inclination angle distribution has increasingly become a trait of interest in terms of its influence on canopy gas and energy exchange processes (e.g. Van Zanten *et al.*, 2010; Mantilla-Perez and Salas Fernandez, 2017; Pisek *et al.*, 2022). For instance, land surface models can represent temperate and boreal broadleaf forests as canopies that tend to have leaves towards the horizontal direction rather than assuming a spherical leaf inclination angle distribution (Bonan *et al.*, 2011). This study provided additional insight into the effect of leaf inclination angle anisotropy on canopy transpiration and WUE. The largest impacts of leaf inclination angle distribution on light interception occurred when LAI was small and on photosynthesis and WUE when LAI was high. When LAI is small (e.g. young canopy), the largest gains in light interception and photosynthesis are attained by increasing LAI, although this comes at an increasingly expensive water cost. As the canopy develops, there are diminishing returns on increasing LAI, and leaf angle becomes increasingly important for productivity. A transition to more vertical leaf angle distribution at this point might be beneficial not only in terms of increasing photosynthesis, but also WUE. Daily photosynthesis varied by 39 % and daily WUE by 36 % across all leaf angle distributions considered when LAI = 5.

It is also noteworthy that daily transpiration varied between all cases considered by <10 % relative to the corresponding spherical leaf angle distribution case, whereas daily photosynthesis and WUE could vary by >30 %. This is probably attributable to the fact that the difference in relative transpiration rate between a leaf perpendicular and parallel to the sun is much smaller than for relative photosynthesis.

Leaf azimuthal angle anisotropy

Anisotropy in leaf azimuth is rarely considered in models or field experiments, although it can have a similar impact as anisotropy in leaf inclination. Previous work has illustrated that leaf azimuthal anisotropy can amplify the effects of canopy heterogeneity (Ponce de León and Bailey, 2019). For instance, in row-oriented canopies, the effective path length of the sun's rays through vegetation can change dramatically with changes in sun azimuth, which is important in agricultural canopy design applications, such as to reduce the effect of elevated temperatures in vineyards (Ponce de León and Bailey, 2022). The present work also explored the effect of leaf azimuth on canopy biophysical processes. In canopies with high LAI, simulation results suggested that biasing leaf normals towards the N–S directions in an erectophile canopy increased A_c and WUE_c by ~30 % relative to E–W biased leaves. This finding is consistent with field experiments that reported a ~25 and ~22 % increase in A_c and WUE_c, respectively, for vertical leaves biased towards N–S compared with E–W (Smith and Ullberg, 1989).

For canopy-level models applied to sparse natural canopies or row-oriented crops, consideration of leaf azimuthal anisotropy within radiation attenuation coefficients might have an important effect on model predictions, particularly in canopies with leaf inclination tending towards vertical. Although leaf (inclination) angle has become a trait of increasing interest for ecosystem ecology, plant physiology and remote sensing (e.g. Pisek *et al.*, 2022; Yang *et al.*, 2023), measurement and consideration of leaf azimuth might warrant attention in addition to the more common practice of measuring leaf inclination angle only (e.g. Daviet *et al.*, 2022; Serouart *et al.*, 2023). Fortunately, techniques now exist for high-throughput measurement of leaf inclination and azimuth from LiDAR scanning data (e.g. Bailey and Mahaffee, 2017) and from accelerometers integrated within leaf-level measurement devices, such as the LICOR LI-600 porometer (LICOR Biosciences, Lincoln, NE, USA).

Canopy heterogeneity

The results suggested that canopy heterogeneity can have a significant effect on biophysical processes related to WUE, yet the majority of plant system models are based on assumptions of canopy homogeneity or include heterogeneity through empirically tunable parameters (e.g. Sellers *et al.*, 1992; Sykes *et al.*, 2001; Lawrence *et al.*, 2019). The least heterogeneous discontinuous canopy case considered was still relatively homogeneous, with a crown ground cover fraction of 78 %. Nevertheless, this amount of heterogeneity decreased E_c by ~36 % and increased WUE_c by ~88 %. The effect of adding this small amount of heterogeneity was minimal for A_c owing to offsetting effects of the increase in light distribution efficiency and decrease in total leaf area. The impact of heterogeneity on WUE_c for plant spacing larger than 2:1 was minimal, because at this point the crowns were almost fully isolated, and WUE is not impacted by reduction in leaf area on a ground area basis because it is a ratio.

Linkage between leaf area, leaf angle distribution and heterogeneity

By and large, the effect of increasing LAI, increasing G_{avg} and increasing homogeneity (at constant leaf area density) had a similar effect on daily-integrated canopy fluxes. Variation of these parameters in this way generally leads to increased light interception owing to the resulting increase in projected leaf area. This tends to increase canopy photosynthesis at low LAI, primarily because of the increase in total light available to the canopy, and decreases canopy photosynthesis at high LAI owing to inefficient utilization of light throughout the canopy depth. This additional light increases canopy transpiration owing to additional available energy and transpiring surface area in the case of increasing LAI. Increased light interception tended to cause a monotonic decrease in WUE_c.

Limitations and future work

A limitation of the proposed study is the lack of direct experimental validation. However, it is extremely difficult to vary interacting parameters systematically within field experiments. Natural variation in canopy structure over time or space will inherently be confounded by associated changes in environmental or physiological variables, not to mention that reliably measuring the variables associated with this canopy structure is difficult. Measurement of canopy-scale WUE is additionally difficult, owing to non-vegetative and non-local contributions to water vapour and CO_2 fluxes. In this study, the simulated data were generated by a 3D leaf-resolving model, in which the exact inputs were known. Each of the model sub-components is physically based and has been validated independently. Virtual experiments establish a theoretical basis for guiding field experiments and future reduced-order modelling studies, which could be expanded to short- and long-term leaf responses of WUE to environmental conditions. For instance, studying the leaf response to elevated temperatures or droughts could provide valuable information for breeding climate-resilient cultivars.

In real canopies, plant architectural and physiological traits vary with height and laterally within the canopy owing to structural heterogeneity (Niinemets, 1998, 2010; Buckley *et al.*, 2013; Raabe *et al.*, 2015). In order to make the present study tractable, leaf area density, leaf angle distribution, radiative properties and physiological parameters were assumed constant in space. There is no doubt that including such variation would impact results, but the underlying principles are expected to be the same. The models used in this work are fully capable of representing arbitrarily complex spatial distributions of these traits, which could be used as a tool for future exploration of how these traits are distributed in real canopies and how this impacts canopy-scale fluxes.

Only a single representative weather scenario without diffuse solar radiation, and a single location, was considered, although it is known that weather and geographical conditions can have a significant impact on WUE (Tan *et al.*, 2015; Dekker *et al.*, 2016). Because of the large number of variables already considered in this work, it was not possible also to explore in depth the effects of different weather scenarios and geographical conditions. Although it is clear that variation in specified weather inputs would have a significant effect on the magnitude of fluxes related to WUE, it is expected that overall trends should hold for a wide range of conditions. Extreme conditions that cause near stomatal closure, excessively high respiration rates or very small photosynthetic rates owing to cold temperatures, for example, could cause transitional behaviour. If the canopy location was chosen to be at a different latitude, this would affect the day length and minimum solar zenith angle, which could have an effect on daily integrated fluxes. For example, at higher latitudes the daily light interception is expected to increase in the erectophile canopies and decrease in the planophile canopies. It is expected that addition of diffuse radiation should decrease the impact of the leaf angle distribution, because leaf angle has no impact when incident radiation is isotropic. Further work is needed to explore whether and when weather and geographical conditions can cause transitional behaviour in the interactions between WUE and canopy architecture.

Conclusion

The results showed that variations in leaf area and leaf angle could have a substantial effect on WUE and that the effect of leaf angle increases as canopy density increases or heterogeneity decreases. There was no observed optimum in WUE as LAI, the leaf angle distribution or heterogeneity was varied. There was, however, an optimum in daily canopy photosynthesis with increasing light interception owing to the trade-off between the increase in photosynthesis with increasing available light and the decrease in photosynthesis owing to respiratory costs of shaded leaf area. It can thus be concluded that leaf angle and density traits might be viable targets for increasing crop productivity through breeding or through management practices, such as pruning and thinning. Results suggested that in dense canopies, reduction in vegetation density through thinning or biasing leaf angles towards the vertical could simultaneously increase photosynthesis and WUE. Furthermore, the potentially high impact of these architectural traits on WUE motivates their explicit representation within land

surface models, and their accurate specification as model inputs. More work is needed to investigate thoroughly leaf solar tracking or other traits that could permit optima in WUE with varying architecture.

SUPPLEMENTARY DATA

Supplementary data are available at *Annals of Botany* online and consist of the following.

Figure S1: theoretical and calculated (Helios) whole-canopy fluxes of PAR interception (Q) on Julian day 153. Figure S2: theoretical and calculated (Helios) fraction of sunlit leaf area (fsun) on Julian day 153. Table S1: model performance metrics for the four different leaf inclination distributions in a homogeneous canopy with isotropic leaf azimuth.

FUNDING

This work was supported by the United States Department of Agriculture National Institute of Food and Agriculture, Hatch project number 1013396, and United States National Science Foundation grant IOS 2047628.

LITERATURE CITED

Bailey BN. 2018. A reverse ray-tracing method for modelling the net radiative flux in leaf-resolving plant canopy simulations. *Ecological Modelling* **368**: 233–245.

Bailey BN. 2019. Helios: a scalable 3D plant and environmental biophysical modeling framework. *Frontiers in Plant Science* **10**: 1185.

Bailey BN, **Kent ER. 2021**. On the resolution requirements for accurately representing interactions between plant canopy structure and function in three-dimensional leaf-resolving models. *In Silico Plants* **3**: diab023.

Bailey BN, **Mahaffee WF. 2017**. Rapid measurement of the three-dimensional distribution of leaf orientation and the leaf angle probability density function using terrestrial lidar scanning. *Remote Sensing of Environment* **194**: 63–76.

Bernacchi C, **Singsaas E**, **Pimentel C**, **Portis A Jr**, **Long S. 2001**. Improved temperature response functions for models of Rubisco-limited photosynthesis. *Plant, Cell & Environment* **24**: 253–259.

Bernacchi C, **Pimentel C**, **Long SP. 2003**. *In vivo* temperature response functions of parameters required to model RuBP-limited photosynthesis. *Plant, Cell & Environment* **26**: 1419–1430.

Bonan GB, **Lawrence PJ**, **Oleson KW**, ***et al***. **2011**. Improving canopy processes in the Community Land Model version 4 (CLM4) using global flux fields empirically inferred from FLUXNET data. *Journal of Geophysical Research, Biogeosciences* **116**: G02014.

Buckley TN, **Turnbull TL**, **Adams MA. 2012**. Simple models for stomatal conductance derived from a process model: cross-validation against sap flux data. *Plant, Cell & Environment* **35**: 1647–1662.

Buckley TN, **Cescatti A**, **Farquhar GD. 2013**. What does optimization theory actually predict about crown profiles of photosynthetic capacity when models incorporate greater realism? *Plant, Cell & Environment* **36**: 1547–1563.

Campbell GS, **Norman JM. 1998**. Radiation fluxes in natural environments. In: **Campbell GS**, **Norman JM.** eds. *An introduction to environmental biophysics*. New York, USA: Springer, 167–184.

Chelle M, **Andrieu B. 1998**. The nested radiosity model for the distribution of light within plant canopies. *Ecological Modelling* **111**: 75–91.

Condon AG, **Richards RA**, **Rebetzke GJ**, **Farquhar GD. 2004**. Breeding for high water-use efficiency. *Journal of Experimental Botany* **55**: 2447–2460.

Daviet B, **Fernandez R**, **Cabrera-Bosquet L**, **Pradal C**, **Fournier C. 2022**. PhenoTrack3D: an automatic high-throughput phenotyping pipeline to track maize organs over time. *Plant Methods* **18**: 130.

Dekker SC, **Groenendijk M**, **Booth BB**, **Huntingford C**, **Cox PM. 2016**. Spatial and temporal variations in plant water-use efficiency inferred from tree-ring, eddy covariance and atmospheric observations. *Earth System Dynamics* **7**: 525–533.

De Pury D, **Farquhar G. 1997**. Simple scaling of photosynthesis from leaves to canopies without the errors of big-leaf models. *Plant, Cell & Environment* **20**: 537–557.

de Wit CT. 1965. *Photosynthesis of Leaf Canopies*. Wageningen, The Netherlands: Agricultural Research Report 663. 57.

Digrado A, **Mitchell NG**, **Montes CM**, **Dirvanskyte P**, **Ainsworth EA. 2020**. Assessing diversity in canopy architecture, photosynthesis, and water-use efficiency in a cowpea magic population. *Food and Energy Security* **9**: e236.

Drewry DT, **Kumar P**, **Long SP. 2014**. Simultaneous improvement in productivity, water use, and albedo through crop structural modification. *Global Change Biology* **20**: 1955–1967.

Ehleringer J, **Werk K. 1986**. Modifications of solar-radiation absorption patterns and implications for carbon gain at the leaf level. In: On the economy of plant form and function: proceedings of the Sixth Maria Moors Cabot Symposium, Evolutionary Constraints on Primary Productivity, Adaptive Patterns of Energy Capture in Plants, Harvard Forest, August 1983. Cambridge, UK: Cambridge University Press, 57–82.

Ezcurra E, **Montaña C**, **Arizaga S. 1991**. Architecture, light interception, and distribution of *Larrea* species in the Monte Desert, Argentina. *Ecology* **72**: 23–34.

Falster DS, **Westoby M. 2003**. Leaf size and angle vary widely across species: what consequences for light interception? *The New Phytologist* **158**: 509–525.

Farquhar GD, **von Caemmerer S**, **Berry JA. 1980**. A biochemical model of photosynthetic CO_2 assimilation in leaves of C_3 species. *Planta* **149**: 78–90.

Foley JA, **Prentice IC**, **Ramankutty N**, ***et al***. **1996**. An integrated biosphere model of land surface processes, terrestrial carbon balance, and vegetation dynamics. *Global Biogeochemical Cycles* **10**: 603–628.

Forrester, DI, **Collopy JJ**, **Beadle CL**, **Warren CR**, **Baker TG. 2012**. Effect of thinning, pruning and nitrogen fertiliser application on transpiration, photosynthesis and water-use efficiency in a young *Eucalyptus nitens* plantation. *Forest Ecology and Management* **266**: 286–300.

Forseth I, **Ehleringer J. 1983**. Ecophysiology of two solar tracking desert winter annuals. *Oecologia* **58**: 10–18.

Goel NS, **Strebel DE. 1984**. Simple beta distribution representation of leaf orientation in vegetation canopies. *Agronomy Journal* **76**: 800–802.

Gueymard CA. 2008. REST2: high-performance solar radiation model for cloudless-sky irradiance, illuminance, and photosynthetically active radiation – validation with a benchmark dataset. *Solar Energy* **82**: 272–285.

Hatfield JL, **Dold C. 2019**. Water-use efficiency: advances and challenges in a changing climate. *Frontiers in Plant Science* **10**: 103.

Henke M, **Buck-Sorlin GH. 2017**. Using a full spectral raytracer for calculating light microclimate in functional-structural plant modelling. *Computing and Informatics* **36**: 1492–1522.

Humphries S, **Long S. 1995**. WIMOVAC: a software package for modelling the dynamics of plant leaf and canopy photosynthesis. *Bioinformatics* **11**: 361–371.

James SA, **Bell DT. 2000**. Leaf orientation, light interception and stomatal conductance of *Eucalyptus globulus* ssp. *globulus* leaves. *Tree Physiology* **20**: 815–823.

Jin S, **Wang Y**, **Shi L**, **Guo X**, **Zhang J. 2018**. Effects of pruning and mulching measures on annual soil moisture, yield, and water use efficiency in jujube (*Ziziphus jujube* Mill.) plantations. *Global Ecology and Conservation* **15**: e00406.

Jones C, **Dyke P**, **Williams J**, **Kiniry J**, **Benson V**, **Griggs R. 1991**. EPIC: an operational model for evaluation of agricultural sustainability. *Agricultural Systems* **37**: 341–350.

Jones JW, **Hoogenboom G**, **Porter CH**, ***et al***. **2003**. The DSSAT cropping system model. *European Journal of Agronomy* **18**: 235–265.

Kao WY, **Forseth I. 1992**. Diurnal leaf movement, chlorophyll fluorescence and carbon assimilation in soybean grown under different nitrogen and water availabilities. *Plant, Cell & Environment* **15**: 703–710.

Kao WY, **Tsai TT**, **Chen WH. 1998**. Response of photosynthetic gas exchange and chlorophyll a fluorescence of *Miscanthus floridulus* (Labill) Warb. to temperature and irradiance. *Journal of Plant Physiology* **152**: 407–412.

Knauer J, **Zaehle S**, **Medlyn BE**, ***et al***. **2018**. Towards physiologically meaningful water-use efficiency estimates from eddy covariance data. *Global Change Biology* **24**: 694–710.

Kustas WP, **Norman JM. 1999**. Evaluation of soil and vegetation heat flux predictions using a simple two-source model with radiometric temperatures for partial canopy cover. *Agricultural and Forest Meteorology* **94**: 13–29.

Lawrence DM, **Fisher RA**, **Koven CD**, ***et al***. **2019**. The Community Land Model version 5: description of new features, benchmarking, and impact of forcing uncertainty. *Journal of Advances in Modeling Earth Systems* **11**: 4245–4287.

Le Roux X, **Bariac T**, **Sinoquet H**, ***et al***. **2001**. Spatial distribution of leaf water-use efficiency and carbon isotope discrimination within an isolated tree crown. *Plant, Cell & Environment* **24**: 1021–1032.

Liu T, **Gu L**, **Dong S**, **Zhang J**, **Liu P**, **Zhao B. 2015**. Optimum leaf removal increases canopy apparent photosynthesis, ^{13}C-photosynthate distribution and grain yield of maize crops grown at high density. *Field Crops Research* **170**: 32–39.

Lloyd J, **Grace J**, **Miranda AC**, ***et al***. **1995**. A simple calibrated model of Amazon rainforest productivity based on leaf biochemical properties. *Plant, Cell & Environment* **18**: 1129–1145.

Long S, **Farage P**, **Garcia R. 1996**. Measurement of leaf and canopy photosynthetic CO_2 exchange in the field. *Journal of Experimental Botany* **47**: 1629–1642.

Long SP, **Zhu XG**, **Naidu SL**, **Ort DR. 2006**. Can improvement in photosynthesis increase crop yields? *Plant, Cell & Environment* **29**: 315–330.

López A, **Molina-Aiz F**, **Valera D**, **Peña A. 2012**. Determining the emissivity of the leaves of nine horticultural crops by means of infrared thermography. *Scientia Horticulturae* **137**: 49–58.

Mahaffee WF, **Margairaz F**, **Ulmer LD**, **Bailey BN**, **Stoll R. 2023**. Catching spores: linking epidemiology, pathogen biology, and physics to ground-based airborne inoculum monitoring. *Plant Disease* **107**: 13–33.

Mantilla-Perez MB, **Salas Fernandez MG. 2017**. Differential manipulation of leaf angle throughout the canopy: current status and prospects. *Journal of Experimental Botany* **68**: 5699–5717.

McPherson RA. 2007. A review of vegetation—atmosphere interactions and their influences on mesoscale phenomena. *Progress in Physical Geography: Earth and Environment* **31**: 261–285.

Nelson JA, **Pérez-Priego O**, **Zhou S**, ***et al***. **2020**. Ecosystem transpiration and evaporation: insights from three water flux partitioning methods across fluxnet sites. *Global Change Biology* **26**: 6916–6930.

Niinemets U. 1998. Adjustment of foliage structure and function to a canopy light gradient in two co-existing deciduous trees. Variability in leaf inclination angles in relation to petiole morphology. *Trees* **12**: 446–451.

Niinemets U. 2010. A review of light interception in plant stands from leaf to canopy in different plant functional types and in species with varying shade tolerance. *Ecological Research* **25**: 693–714.

Ort DR. 2001. When there is too much light. *Plant Physiology* **125**: 29–32.

Pearcy RW, **Yang W. 1996**. A three-dimensional crown architecture model for assessment of light capture and carbon gain by understory plants. *Oecologia* **108**: 1–12.

Pisek J, **Diaz-Pines E**, **Matteucci G**, **Noe S**, **Rebmann C. 2022**. On the leaf inclination angle distribution as a plant trait for the most abundant broadleaf tree species in Europe. *Agricultural and Forest Meteorology* **323**: 109030.

Ponce de León MA, **Bailey BN. 2019**. Evaluating the use of Beer's law for estimating light interception in canopy architectures with varying heterogeneity and anisotropy. *Ecological Modelling* **406**: 133–143.

Ponce de León MA, **Bailey BN. 2021**. A 3D model for simulating spatial and temporal fluctuations in grape berry temperature. *Agricultural and Forest Meteorology* **306**: 108431.

Ponce de León MA, **Bailey BN. 2022**. Fruit zone shading to control grape berry temperature: a modeling study. *American Journal of Enology and Viticulture* **73**: 183–197.

Prata A. 1996. A new long-wave formula for estimating downward clear-sky radiation at the surface. *Quarterly Journal of the Royal Meteorological Society* **122**: 1127–1151.

Raabe K, **Pisek J**, **Sonnentag O**, **Annuk K. 2015**. Variations of leaf inclination angle distribution with height over the growing season and light exposure for eight broadleaf tree species. *Agricultural and Forest Meteorology* **214–215**: 2–11.

Richards RA, **Cavanagh CR**, **Riffkin P. 2019**. Selection for erect canopy architecture can increase yield and biomass of spring wheat. *Field Crops Research* **244**: 107649.

Ross J. 1981. *The radiation regime and architecture of plant stands*. The Hague: Dr W. Junk.

Schuepp P. 1993. Tansley review No. 59. Leaf boundary layers. *New Phytologist* **125**: 477–507.

Sellers P, **Berry J**, **Collatz G**, **Field C**, **Hall F. 1992**. Canopy reflectance, photosynthesis, and transpiration. III. A reanalysis using improved leaf models and a new canopy integration scheme. *Remote Sensing of Environment* **42**: 187–216.

Sellers P, **Randall D**, **Collatz G**, ***et al***. **1996**. A revised land surface parameterization (SiB2) for atmospheric GCMs. Part I: model formulation. *Journal of Climate* **9**: 676–705.

Serouart M, **Lopez-Lozano R**, **Daubige G**, ***et al***. **2023**. Analyzing changes in maize leaves orientation due to GxExM using an automatic method from RGB images. *Plant Phenomics* **5**: 0046.

Smith M, **Ullberg D. 1989**. Effect of leaf angle and orientation on photosynthesis and water relations in *Silphium terebinthinaceum*. *American Journal of Botany* **76**: 1714–1719.

Song Q, **Zhang G**, **Zhu XG. 2013**. Optimal crop canopy architecture to maximise canopy photosynthetic CO_2 uptake under elevated CO_2 – a theoretical study using a mechanistic model of canopy photosynthesis. *Functional Plant Biology* **40**: 108–124.

Srinivasan V, **Kumar P**, **Long SP. 2017**. Decreasing, not increasing, leaf area will raise crop yields under global atmospheric change. *Global Change Biology* **23**: 1626–1635.

Sykes MT, **Prentice IC**, **Smith B**, **Cramer W**, **Venevsky S. 2001**. An introduction to the European terrestrial ecosystem modelling activity. *Global Ecology and Biogeography* **10**: 581–593.

Tan Z-H, **Zhang Y-P**, **Deng X-B**, ***et al***. **2015**. Interannual and seasonal variability of water use efficiency in a tropical rainforest: results from a 9 year eddy flux time series. *Journal of Geophysical Research: Atmospheres* **120**: 464–479.

Van Zanten M, **Pons T**, **Janssen J**, **Voesenek L**, **Peeters A. 2010**. On the relevance and control of leaf angle. *Critical Reviews in Plant Science* **29**: 300–316.

Walker AP, **Beckerman AP**, **Gu L**, ***et al***. **2014**. The relationship of leaf photosynthetic traits – V_{cmax} and J_{max} – to leaf nitrogen, leaf phosphorus, and specific leaf area: a meta-analysis and modeling study. *Ecology and Evolution* **4**: 3218–3235.

Wang YP, **Leuning R. 1998**. A two-leaf model for canopy conductance, photosynthesis and partitioning of available energy I: model description and comparison with a multi-layered model. *Agricultural and Forest Meteorology* **91**: 89–111.

Wang Y, **Song Q**, **Jaiswal D**, **de Souza AP**, **Long SP**, **Zhu XG. 2017**. Development of a three-dimensional ray-tracing model of sugarcane canopy photosynthesis and its application in assessing impacts of varied row spacing. *Bioenergy Research* **10**: 626–634.

Watanabe T, **Hanan JS**, **Room PM**, **Hasegawa T**, **Nakagawa H**, **Takahashi W. 2005**. Rice morphogenesis and plant architecture: measurement, specification and the reconstruction of structural development by 3D architectural modelling. *Annals of Botany* **95**: 1131–1143.

Wise RR, **Frederick JR**, **Alm D**, ***et al***. **1990**. Investigation of the limitations to photosynthesis induced by leaf water deficit in field-grown sunflower (*Helianthus annuus* L.). *Plant, Cell & Environment* **13**: 923–931.

Yang X, **Li R**, **Jablonski A**, ***et al***. **2023**. Leaf angle as a leaf and canopy trait: rejuvenating its role in ecology with new technology. *Ecology Letters* **26**: 1005–1020.

Zhuang J, **Chi Y**, **Wang Y**, **Zhou L. 2023**. Trade-off of leaf-scale resource-use efficiencies along the vertical canopy of the subtropical forest. *Journal of Plant Physiology* **286**: 154004.